

Bose-Einstein transition in a dilute interacting gas

 G. Baym^{1,2,3}, J.-P. Blaizot², M. Holzmann^{1,3,a}, F. Laloë³, and D. Vautherin^{4,†}
¹ University of Illinois at Urbana-Champaign, 1110 W. Green St., Urbana, IL 61801, USA

² CEA-Saclay, Service de Physique Théorique, 91191 Gif-sur-Yvette, Cedex, France

³ LKB and LPS, École Normale Supérieure, 24 rue Lhomond, 75005 Paris, France

⁴ LPNHE, Case 200, Universités Paris 6/7, 4 Place Jussieu, 75005 Paris, France

Received 15 July 2001

Abstract. We study the effects of repulsive interactions on the critical density for the Bose-Einstein transition in a homogeneous dilute gas of bosons. First, we point out that the simple mean field approximation produces no change in the critical density, or critical temperature, and discuss the inadequacies of various contradictory results in the literature. Then, both within the frameworks of Ursell operators and of Green's functions, we derive self-consistent equations that include correlations in the system and predict the change of the critical density. We argue that the dominant contribution to this change can be obtained within classical field theory and show that the lowest order correction introduced by interactions is linear in the scattering length, a , with a positive coefficient. Finally, we calculate this coefficient within various approximations, and compare with various recent numerical estimates.

PACS. 05.30.Jp Boson systems – 05.30.-d Quantum statistical mechanics – 03.75.Fi Phase coherent atomic ensembles; quantum condensation phenomena

1 Introduction

A precise description of the role of interparticle correlations on the Bose-Einstein transition is indispensable to understanding its physical nature; indeed, correlations are expected to play an essential role in the very existence of superfluidity and related properties, vortices, flow metastability, etc. In general, dilute systems offer the possibility of accurate microscopic treatments. The study of the Bose-Einstein transition in very dilute gases could provide experimental tests of the theory. A large portion of the literature on the modification of the transition temperature is based on a simple transposition of one of the most popular methods of condensed matter physics, mean field theory in various guises, where the correlations are unmodified by the interactions and remain purely statistical (as in an ideal gas). Mean field theories, for instance Gross-Pitaevskii, successfully describe a broad variety of interesting phenomena observable in experiments, for example the spatial distribution of the gas in a harmonic trap [1,2]; for a recent review of numerous successful applications of mean field theories in Bose-Einstein condensation in atomic gases, see [3]. Our purpose in this paper is to go beyond mean field theories and to explore the effects

of correlations on the properties of the transition, studying in particular how they modify the transition temperature.

We assume that the interparticle interaction can be described by a positive scattering length a , equivalent to the interaction of hard spheres of diameter a . We shall also consider a dilute gas, *i.e.*, work in the regime where a is much smaller than the interparticle distance, $an^{1/3} \ll 1$, where n is the particle density. The critical number density, n_c^0 , of an ideal gas is given by

$$n_c^0 \lambda^3 = \zeta(3/2) \simeq 2.612, \quad (1)$$

where λ is the thermal wavelength

$$\lambda = \frac{h}{\sqrt{2\pi m k_B T}}, \quad (2)$$

ζ the Riemann zeta function; m the particle mass and k_B Boltzmann's constant. Note that since at the transition $\lambda \sim n^{-1/3}$, the diluteness condition is equivalent to $a \ll \lambda$.

In an interacting gas, the critical value of the degeneracy parameter, $n_c \lambda^3$, is modified; the first order change in the critical temperature is related to that in the degeneracy parameter by

$$\frac{\Delta T_c}{T_c^0} = -\frac{2}{3} \frac{\Delta(n_c \lambda^3)}{n_c^0 \lambda^3}. \quad (3)$$

Because mean field theories effectively treat physical systems as ideal gases with modified parameters, the dimensionless degeneracy parameter keeps exactly the same

^a e-mail: holzmann@mail.physics.uiuc.edu

[†] Our friend Dominique passed away on December 6, 2000, before this manuscript was completed

value as in an ideal gas¹. To calculate its change as a function of the interactions it is necessary to go beyond mean field theories and include correlations arising from the interactions.

One might expect repulsive interactions to increase the degeneracy parameter – equivalently, to decrease the critical temperature, T_c , at constant density; in general, the presence of hard cores tends to impede the motion of the particles necessary for quantum exchange effects, therefore reducing the influence of quantum statistics and the critical temperature. For example, the superfluid transition temperature of liquid ^4He is below that of an ideal gas of the same density. Moreover, applying pressure to liquid ^4He effectively increases the role of the repulsive core of the potential, and decreases the critical temperature².

Studies on the effect of interactions on the transition began in the 1950's with the work of Huang, Yang, and Luttinger [5], who concluded that the phase transition of the interacting Bose gas “more closely resembles an ordinary gas-liquid transition than the Bose-Einstein condensation,” but they did not make a specific prediction for the change in T_c . Shortly thereafter Lee and Yang [6] predicted an *increase* of T_c proportional to $a^{1/2}$; later, in reference [7] they corrected this result and concluded that the shift of the critical temperature is linear in a , with no prediction for the magnitude or even the sign of the effect. In 1960, Glassgold *et al.* predicted again a positive temperature shift proportional to $a^{1/2}$ [8]. Later, Huang predicted an increase $\sim a^{3/2}$ [9], and recently [10], he predicted that T_c increases as $a^{1/2}$, using the same virial expansion as that of reference [6]. Despite the lack of qualitative agreement among these many solutions of the problem, these studies showed that the changes in question were not merely due to excluded volume effects (proportional to the cube of the hard core diameter a) but to more interesting quantum effects, proportional to a smaller power of a .

The problem lay dormant for two decades until it was revisited by Toyoda [11], who studied the transition in the Bogoliubov approximation in the condensed phase. This work predicted a *decrease* of the critical temperatures at constant density proportional to $a^{1/2}$. As the sign agreed with the measurements in liquid ^4He , the question appeared settled. Toyoda's result was reinforced by numerical Path-Integral Quantum Monte Carlo calculations showing that the effect of interparticle repulsion was indeed to decrease the critical temperature [12,13]. Nevertheless, at the time of these calculations, the issue did not have the same experimental interest as it has now, and it was not fully appreciated that these calculations were limited to relatively high densities and did not explore the region of dilute systems.

¹ Mean field theories can lead to a change of the effective mass [4], which in turn affects the value of the thermal wavelength in (1); with this effect included, the critical value of the degeneracy parameter remains the same as for the ideal gas.

² In liquid ^3He , the repulsive cores similarly reduce the effect of quantum statistics, so that the magnetic susceptibility is significantly higher than in an ideal Fermi system with the same density.

With the prospect of experimental realization of Bose-Einstein condensation in dilute gases, Stoof [14,15] carried out many-body and renormalization group analyses concentrating on the dilute regime. Stoof's work contains interesting precursors to the present work, *e.g.*, reference [14] predicts a linear positive shift in the critical temperature about twice that of our estimate in [16]. Reference [15] predicts more structure in the a dependence of the effect, $\sim a \ln a$, [17], qualitatively similar to the $a^2 \ln a$ we describe below [18].

A surprise came when the Monte Carlo calculations for hard sphere bosons were extended to lower densities and showed, in addition to the depression of T_c at high densities, the existence of a low density regime where the critical temperature is indeed increased by the interaction [19]. At very low densities the shift of the critical temperature was found to be

$$\frac{\Delta T_c}{T_c^0} = c n^{1/3} a, \quad (4)$$

with $c \simeq 0.34$, determined by a numerical extrapolation to the limit $a \rightarrow 0$. However, a more recent explicit Monte Carlo calculation [20] of the leading correction to the ideal gas behavior predicts a prefactor $c \simeq 2.3$. One source of the discrepancy lies in the non-analytic dependence of T_c on a , discussed below, which gives rise to non-linear corrections at the densities where the Monte Carlo calculation of reference [19] was performed.

In the past several years, the problem was attacked by analytic approaches based on self-consistent non-linear equations derived both in the Ursell operator formalism [21], and the Green's function formalism [16]. One finds in both approaches that the effect of repulsive interactions is to decrease the degeneracy parameter, thus increasing the critical temperature at constant density. Moreover, reference [16] proves the linearity of ΔT_c in a . This was done by observing that the dominant contribution to the shift in the critical density can be calculated by restricting the propagators to their zero Matsubara frequency sector, thereby reducing the quantum many-body problem to a classical field theoretical problem in three spatial dimensions. An alternative proof of the linearity in a based on renormalization group arguments is presented in [22]. While references [16,21,22] all agree on the functional form, they do not provide definitive quantitative predictions for the prefactor; reference [21] provides $c \sim 1$, and an estimate in reference [16] of an exact formula for $\Delta T_c/T_c^0$ predicts $c \sim 2-3$. In the limit of a large number N of components [22], $c = 8\pi/3\zeta(3/2)^{4/3} \simeq 2.33$; interestingly, this exact result for $N \rightarrow \infty$ agrees with the numerical result $c = 2.33 \pm 0.25$ of reference [20] for $N = 2$. The reduction of the problem to classical field theory has been exploited in the recent calculations of the transition in classical ϕ^4 field theory on the lattice extrapolated to the continuum [23,24], which give $c \simeq 1.3$.

The linearity in a is a non-trivial, non-perturbative result. Since the interaction is itself linear in a , one might imagine deriving this result in some form of simple perturbation theory. However, the first order term in a , for

fixed density, vanishes identically, while all higher order terms have infrared divergences. Nonetheless, various authors have attempted to skirt the infrared problems. For example, reference [25] unjustifiably “regularizes” divergences in sums that appear at the transition with an analytic continuation of the Riemann zeta function³. Similarly, reference [10] uses a virial expansion, unjustified at the critical point, as we discuss below. In another approach, reference [26] attempts to exploit differences in first order perturbation theory between the canonical and grand-canonical ensembles in finite volume; this perturbative approach necessarily fails in the thermodynamic limit, preventing a direct determination of the critical temperature. In reference [27] finite-size-scaling is used to reconcile this approach with the grand-canonical calculations. Reference [28] calculates T_c with the help of an “optimized linear delta expansion, which avoids infrared divergences and operates for any N ; for $N = 2$ the authors find $c \sim 3.0$, but the validity of the method is difficult to assess, and the accuracy of this result may be affected by uncontrolled errors.

The aim of this paper is to summarize current understanding of the problem of the transition temperature. We provide a more detailed account of our earlier analytical calculations, and in addition compare the Green’s function and Ursell calculations. The paper is organized as follows: In the next section we recall features of the Bose-Einstein transition in an ideal gas and show how the addition of a mean repulsive field does not alter the critical value of the degeneracy parameter. Then in Section 3 we include correlations and obtain, using alternatively the Ursell and Green’s function formalisms, simple self-consistent equations which reveal the physical origin of the change in the critical temperature. In Section 4 we show that the dominant contribution to the change in the critical temperature can be calculated using a classical field approximation, and we show that the resulting change is linear in the scattering length. Section 5 is devoted to numerical calculations of the coefficient c , and to a numerical exploration of the range of validity of the linear behavior. We focus throughout on a spatially uniform system; a discussion of the transition temperature of a dilute gas in a trap can be found in references [2, 29, 30]. For experimental data in the ⁴He-Vycor system, see [31].

2 Ideal gas, mean field and related calculations

In a homogeneous system, the number density of a non-condensed ideal Bose gas is given by

$$n = \int \frac{d^3k}{(2\pi)^3} \frac{1}{e^{\beta(\varepsilon_k^0 - \mu)} - 1} = \frac{1}{\lambda^3} g_{3/2}(z) \quad (5)$$

³ Indeed, the method of reference [25] applied to the simplest case of the non-interacting Bose gas implies that as μ goes to zero $\partial n / \partial \mu = \lambda^3 \zeta(1/2) / T$, which is finite and negative, in contradiction to the divergence of the compressibility of the ideal gas.

with $\beta = 1/k_B T$, μ is the chemical potential, $z = \exp(\beta\mu)$ the fugacity, and ($\hbar = 1$)

$$\varepsilon_k^0 = k^2 / 2m; \quad (6)$$

the Bose (polylogarithmic) function $g_p(z)$ is defined by

$$g_p(z) \equiv \sum_{j=1}^{\infty} \frac{z^j}{j^p}. \quad (7)$$

As μ tends to zero from negative values $g_{3/2}(z) \rightarrow \zeta(3/2)$ corresponding to the maximum density for a non-condensed gas at a given temperature given by equation (1).

The simplest way to include repulsive interactions is in mean field. Assuming that all the effects of interactions can be described by an s -wave scattering length, one can generalize equation (5) by writing:

$$n = \frac{1}{\lambda^3} g_{3/2}(e^{\beta(\mu - \Delta\mu)}) \quad (8)$$

where the shift of the chemical potential $\Delta\mu$ is proportional to the number density:

$$\beta\Delta\mu = 2gn\beta = 4a\lambda^2 n, \quad (9)$$

and $g = 4\pi\hbar^2 a / m$. Equation (8) is a simple consequence of the Hartree-Fock approximation, using a pseudopotential proportional to a , in which the shift of the single particle energies is given by

$$\Sigma_{\text{HF}} = 2gn; \quad (10)$$

the factor of two comes from exchange. Since Σ_{HF} is independent of momentum we have to increase the chemical potential by $\Delta\mu = \Sigma_{\text{HF}}$ to keep the same particle density as the ideal gas. The same results are obtained in Section 4 of reference [21].

Because the Hartree-Fock self-energy depends on the density, the relation between the chemical potential at the transition and the critical density is more complicated than in the non-interacting case, and the equation $\mu - \Delta\mu = 0$ is non-linear. Its solution is conveniently obtained with the geometrical method of [21], illustrated in Figure 1. At fixed μ and β , with $\beta\Delta\mu$ as a variable, the density is obtained through (8); then a simple construction provides the value of $\Delta\mu$ corresponding to the transition. Finally, the density as a function of μ varies as shown in Figure 2 (full line); it behaves similarly to that of the ideal gas. However, the transition now occurs at a positive value of the chemical potential and the compressibility $(1/n^2)\partial n / \partial \mu$ is finite, in contrast to the ideal gas where it diverges. As mentioned in the introduction, the critical density remains exactly the same as for the ideal gas, because at the transition $\mu = \Delta\mu$ and thus the critical density is given by the same integral as for the ideal gas.

It is instructive to use this simple mean field model to test the limit of simple approximations in an exactly

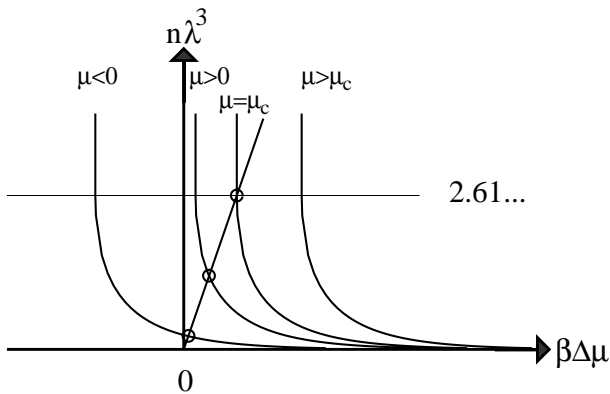


Fig. 1. Plot of the density $n\lambda^3$ as a function of the shift of the chemical potential $\beta\Delta\mu$, for different values of the chemical potential $\beta\mu$. For a given value of $\beta\mu$, the self-consistent solution is given by the intersection point (circle) of this curve with the straight line $\beta\Delta\mu = 4a\lambda^2 n$.

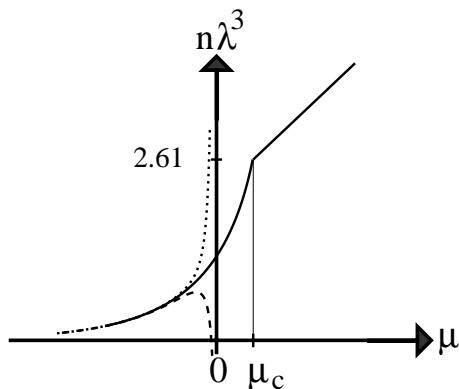


Fig. 2. Variations of the density $n\lambda^3$ as a function of the chemical potential predicted in mean field (full line), for small constant value of the interaction parameter a/λ . The dotted line corresponds to the ideal gas. The mean field solution curve shows no maximum, but a constantly increasing density as a function of the chemical potential. On the other hand, any finite expansion in orders of a/λ leads to divergences around $\mu = 0$ and may introduce spurious extrema (dashed line).

soluble case. Expanding the right side of equation (8) in powers of a/λ we find the virial expansion:

$$n\lambda^3 = g_{3/2}(z) - 4\frac{a}{\lambda}g_{1/2}(z)g_{3/2}(z) + 8\left(\frac{a}{\lambda}\right)^2 g_{3/2}(z) \left\{ 2 [g_{1/2}(z)]^2 + g_{3/2}(z)g_{-1/2}(z) \right\} + \dots \quad (11)$$

Now, if as reference [10] we consider only the first two terms of the expansion we find that the density (the broken lines in Fig. 2) develops a maximum for a negative value of μ ; since the density must always be an increasing function of μ , it then becomes tempting to infer that a phase transition should take place at this point. As seen in the figure, this point corresponds to a smaller density than for the ideal gas; this reasoning would then predict an increase of the critical temperature, at constant density,

proportional to \sqrt{a} , precisely the result obtained in [10]. But one should keep in mind that in this simple model the density maximum is just an artefact of the first order virial expansion, as illustrated by the absence of any maximum in the full curve of Figure 2; in fact, inclusion of second order terms in a of (11) makes the maximum disappear⁴. From the original equation (7), the critical density cannot change. Similar arguments were already given in references [32] and [21]; sufficiently close to $\mu = 0$, higher order terms diverge faster and, eventually, dominate the lower order terms in any virial expansion⁵.

The simple example above illustrates the dangers of truncating an expansion in a , even within the mean field approximation. The physical origin of the difficulty is simple: the very essence of Bose-Einstein condensation is the appearance of long exchange cycles over the system, which cluster together all particles that they contain [35]; therefore, the phenomenon is not easily captured within any formalism containing a limitation on the size of clusters; further discussion of the effect of long exchange clusters on the position of the Bose-Einstein transition can be found in [19]. One must be very careful in truncating perturbative expansions in which nominally higher-order terms turn out to be of comparable order; rather it is necessary in general to sum an infinite number of terms.

In the calculation of Toyoda [11], the only mean field taken into account is that due to the condensed particles below the transition temperature. His approximation is in fact lowest order Bogoliubov theory. While this theory describes correctly the ground state at zero temperature and its elementary excitations, its extension near the critical temperature meets several difficulties; in particular it predicts a first order phase transition [33], a point not taken into account. In fact, above T_c , Toyoda's calculation of the free energy is just that of an ideal gas, with no shift in the critical temperature.

3 Self-consistent equations

In this section, as well as in the rest of this paper, we concentrate on the non-condensed state and approach the critical temperature from above. As we have seen in the previous section, mean field effects which produce merely a constant shift in the single particle energies around T_c do not affect the value of the critical temperature. A modification of T_c thus requires the inclusion of correlations; whose effect of such correlations is to lower the single particle occupation at small k . Thus, as the temperature is

⁴ The second order terms given in reference [10] differ from those of equation (11); nevertheless they do not change our argument.

⁵ The end of the discussion of Section 3.3 of reference [32] was given specifically for the case of attractive interactions; then, instead of a density maximum, the naive first order virial correction model predicts the disappearance of the transition, which is replaced by a simple crossover between two regimes. For repulsive interactions, the sign of the first order correction is opposite, and the density maximum occurs as in reference [10].

lowered, the chemical potential reaches the lowest single particle energy for a value smaller than in mean field, resulting in a decrease of n_c .

It is instructive at this stage to consider the highly oversimplified model in which correlations push down only the level $k = 0$ and all other levels are treated within mean field. Then, at the transition, when the $k = 0$ level hits the chemical potential, the other particles experience a constant energy shift $\bar{\mu} > 0$ with respect to the level $k = 0$, and the critical density is given by:

$$n_c = \int \frac{d^3k}{(2\pi)^3} \frac{1}{e^{\beta(\varepsilon_k^0 + \bar{\mu})} - 1} = \frac{1}{\lambda^3} g_{3/2}(e^{-\beta\bar{\mu}}). \quad (12)$$

Since $\bar{\mu}$ is small, one can expand the Bose function $g_{3/2}(e^{-\beta\bar{\mu}})$:

$$g_{3/2}(e^{-\beta\bar{\mu}}) = \zeta(3/2) - 2\sqrt{\pi\beta\bar{\mu}}. \quad (13)$$

In fact, in calculating the change in the critical density $\Delta n_c = n_c - n_c^0$, one can equivalently expand the statistical factor in (12) at small k :

$$\frac{1}{e^{\beta(\varepsilon_k^0 + \bar{\mu})} - 1} \rightarrow \frac{1}{\beta(\varepsilon_k^0 + \bar{\mu})} \quad (14)$$

and arrive at the result:

$$\begin{aligned} \Delta n_c &= n_c - n_c^0 \approx \int_0^\infty \frac{dk}{\pi^2} \frac{m}{\beta} k^2 \left(\frac{1}{k^2 + 2m\bar{\mu}} - \frac{1}{k^2} \right) \\ &= -\frac{2}{\lambda^3} \sqrt{\pi\beta\bar{\mu}}. \end{aligned} \quad (15)$$

We shall often use the approximation (14) in the following. We note here that it is valid provided only momenta $k \ll \lambda^{-1}$ contribute significantly to the integral (15), which requires $\sqrt{2m\bar{\mu}} \ll \lambda^{-1}$. Since we expect the first correction beyond mean field to be $\beta\bar{\mu} \sim (a/\lambda)^2$, this condition is satisfied if $a \ll \lambda$.

As anticipated, the correlations that push down the level $k = 0$ lead to a decrease of the critical density, and hence to an increase of the critical temperature. Furthermore, the magnitude of the effect is not necessarily analytic in the small change $\bar{\mu}$ of the chemical potential, and hence in the interaction strength a . In fact, the expected result $\beta\bar{\mu} \sim (a/\lambda)^2$ together with equation (15) lead to $\Delta n_c/n_c \sim a/\lambda$. To include correlations more generally we consider two approaches, that of Ursell operators used already for this problem in [21], and that of finite temperature field theory. Before deriving detailed results, let us spend a moment comparing the two approaches.

Within finite temperature field theory one typically carries out a systematic expansion of the properties of a many-body system, *e.g.*, the pressure, in powers of the interaction V , using either unperturbed Green's functions G_0 or self-consistent ones, G . Ursell operators provide a different approach to calculating thermodynamic properties of an interacting many-particle system, and lead naturally to expansions in terms of correlations of higher and higher orders. The Ursell operator of rank n ,

U_n , describes the correlations of a system of n interacting Boltzmann particles. For example, the operator U_2 , defined by

$$U_2 = e^{-\beta(p_1^2/2m + p_2^2/2m + V(r_1 - r_2))} - e^{-\beta(p_1^2/2m + p_2^2/2m)}, \quad (16)$$

accounts for two-body correlations. One expects that matrix elements of U_n vanish between states in which one of the particles is far away from the others, and, in the tradition of cluster expansions, one writes expansions of thermodynamic functions in powers of the Ursell operators U_n . Every term of such an expansion is expected to be finite, even for highly singular potentials such as hard spheres. Inclusion of the specific bosonic or fermionic statistics gives rise to exchange cycles.

Solved exactly, both formalisms give in principle identical results for static thermodynamic properties, and detailed comparisons of how specific approximations can be formulated in either approach can be found in [34]. In the following we study the effects of correlations by means of a simple self-consistent approximation which can be derived in either formalism. This simple self-consistent approximation leads to a nonanalytic change in the spectrum at small k .

3.1 Ursell operators

We briefly summarize the principal results obtained in [21] with the Ursell method, reformulated here in a way to make a ready comparison with the Green's function approach. More details are given in the Appendix.

Reference [21] provides the general diagrammatic rules to obtain the reduced one-body density operator in momentum space, ρ_k , as a function of the ideal gas Bose distribution, f_k , and the Ursell operators U_n ($n \geq 2$). Quite generally, above the critical point the single particle density operator has the form of a Bose distribution, but with modified single particle energies⁶,

$$\rho_k = f_k(\mu - \delta\mu_k) = \frac{1}{e^{\beta(\varepsilon_k^0 + \delta\mu_k - \mu)} - 1}. \quad (17)$$

The particle number density is given in terms of ρ_k by

$$n = \int \frac{d^3k}{(2\pi)^3} \rho_k. \quad (18)$$

When looking for leading order corrections one can safely ignore Ursell operators, U_n , with $n \geq 3$. The resulting topological structure of the diagrams of the Ursell perturbation series then becomes equivalent to that of the

⁶ Since $\delta\mu_k$ is real and plays the role of correcting the ideal gas energy in the Bose distribution, the energies $k^2/2m + \delta\mu_k$ may be regarded as those of statistical quasiparticles, in the sense of reference [36] for the Fermi liquid. Such statistical quasiparticles are not equivalent to those obtained from the Green's functions.

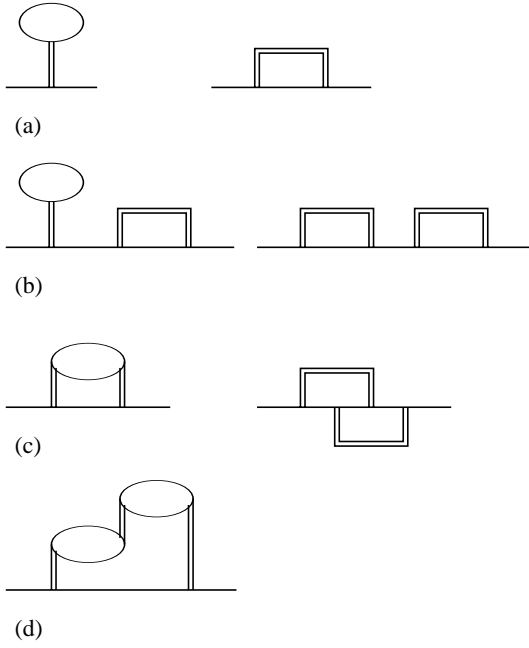


Fig. 3. (a) First order Ursell diagrams; the double line corresponds to one operator U_2 . Here we slightly change the representation of reference [21] and replace the dotted segments there (corresponding to a summation over all exchange cycle lengths) by closed curves; in this way, the U_2 diagrams become very similar to the usual Green's function diagrams. Despite this close graphical similarity, the physical interpretation of the diagrams is different: for instance, exchange cycles do not appear at all in Green's function diagrams. (b) Simplest examples of the diagrams included in the iteration. (c) Diagrams leading to equations (24) and (106). (d) Bubble diagrams leading to equation (109).

perturbative expansion using Green's functions with two-body interactions. Furthermore, by treating the matrix elements of U_2 as momentum independent, one quantitatively recovers the perturbation theory of the Green's function approach with a momentum-independent coupling constant related to the s -wave scattering length a . Finally, as we shall see below, at the critical point the density operator ρ_k becomes large at small momenta, $\rho_k \gg 1$ for $k \rightarrow 0$, so that the approximation

$$1 + \rho_k \simeq \rho_k \simeq [\beta(\varepsilon_k^0 + \delta\mu_k - \mu)]^{-1} \quad (19)$$

can be used systematically (as in (29) below). These remarks explain why the results that we obtain using Ursell operators will eventually be identical to those obtained within the Green's function approach in the particular limit of $a \ll \lambda$.

To obtain the mean field result, equation (32) of reference [21], we iterate the first order diagrams shown in Figure 3a (examples of iterated diagrams are shown in Fig. 3b); this leads to:

$$\rho_k = f_k(\mu - \Delta\mu), \quad (20)$$

with

$$\beta\Delta\mu \simeq 4a\lambda^2 \int \frac{d^3k}{(2\pi)^3} \rho_k = 4a\lambda^2 n. \quad (21)$$

In this approximation the only effect of the interactions is to produce a momentum independent shift of the single particle energies which, as discussed in the previous section, can be absorbed in a shift of the chemical potential:

$$\mu' = \mu - \Delta\mu, \quad (22)$$

leaving the critical density identical to that of the ideal gas.

To go beyond mean field, we include in the self-consistent equation for ρ the corrections displayed in Figure 3c. These are formally of second order in a/λ and read (Sect. 5 of [21]):

$$\rho_k = f_k(\mu' - \delta\mu_k), \quad (23)$$

with

$$\beta\delta\mu_k \simeq -8 \left(\frac{a}{\lambda}\right)^2 \lambda^6 \int \frac{d^3k'}{(2\pi)^3} \int \frac{d^3q}{(2\pi)^3} \rho_{k'} \rho_{k'-q} \rho_{k+q}. \quad (24)$$

Note how the integral (24), in which momentum conservation appears explicitly (q is the momentum transfer in a binary collision), introduces a k -dependence of the energy shift, as opposed to the result of the simple mean field approximation.

We assume that the single particle state with $k = 0$ still has the lowest energy, so that the phase transition occurs when

$$\mu' - \delta\mu_{k=0} = 0. \quad (25)$$

The critical density is then given by

$$n_c = \int \frac{d^3k}{(2\pi)^3} \rho_k = \int \frac{d^3k}{(2\pi)^3} f_k(\delta\mu_{k=0} - \delta\mu_k), \quad (26)$$

which, because of the k -dependence of $\delta\mu_k$, does not coincide with the critical density of the ideal gas obtained for constant $\delta\mu$. Instead

$$\Delta n_c = n_c - n_c^0 = \int \frac{d^3k}{(2\pi)^3} [f_k(\delta\mu_{k=0} - \delta\mu_k) - f_k(\delta\mu_{k=0})]. \quad (27)$$

In general, $\delta\mu_k - \delta\mu_{k=0}$ is an increasing function of k , so that Δn_c is negative.

The variable appearing in equation (26),

$$\delta\mu_k - \delta\mu_{k=0} \simeq -\frac{8}{\beta} \left(\frac{a}{\lambda}\right)^2 \lambda^6 \int \frac{d^3k'}{(2\pi)^3} \times \int \frac{d^3q}{(2\pi)^3} \rho_{k'} \rho_{k'-q} [\rho_{k+q} - \rho_q], \quad (28)$$

can be simplified if we notice that when the critical condition (25) is fulfilled the dominant contribution to the integrals comes from small momenta for which the statistical factors f_k diverge. In fact, if the f_k 's are evaluated with the free particle spectrum, the integral in (24) becomes logarithmically divergent in the infrared. To see that, we expand the f_k 's as in (14),

$$\left[e^{\beta(\varepsilon_k^0 - \mu' + \delta\mu_k)} - 1 \right]^{-1} \simeq \frac{1}{\beta(\varepsilon_k^0 + \delta\mu_k - \mu')}. \quad (29)$$

Setting

$$\varepsilon_k = \varepsilon_k^0 + \delta\mu_k - \delta\mu_{k=0}, \quad (30)$$

we obtain the self-consistent relation valid at small k ,

$$\varepsilon_k = \varepsilon_k^0 - 8 \left(\frac{a\lambda^2}{\beta^2} \right)^2 \int \frac{d^3k'}{(2\pi)^3} \times \int \frac{d^3q}{(2\pi)^3} \frac{1}{\varepsilon_{k'}} \frac{1}{\varepsilon_{k'-q}} \left[\frac{1}{\varepsilon_{k+q}} - \frac{1}{\varepsilon_q} \right]. \quad (31)$$

A simple power counting argument indicates the integral is logarithmically divergent if we replace the self-consistent energies ε by the free ε_k^0 . For the self-consistent spectrum, however, no infrared divergences occur, as we shall see in Section 3.3.

3.2 Green's functions

In the normal state the single particle Green's function $G(k, z_\nu)$ is given

$$G^{-1}(k, z_\nu) = z_\nu + \mu - \varepsilon_k^0 - \Sigma(k, z_\nu), \quad (32)$$

where k is the single particle momentum, and $z_\nu = 2\pi i\nu/\beta$ is a Matsubara frequency, with $\nu = 0, \pm 1, \pm 2, \dots$. The self-energy $\Sigma(k, z)$, which describes the effect of the interactions, can be obtained as a series in powers of the interaction strength a by standard diagrammatic techniques [4, 37–39]. The single particle density matrix is related to G by

$$\rho_k = -T \sum_\nu e^{z_\nu 0^+} G(k, z_\nu). \quad (33)$$

The criterion for condensation is that the chemical potential μ reaches the bottom of the single particle excitation spectrum, and we again assume, as in Section 3.1, that the lowest single particle state is that with $k = 0$. The transition point is then determined by the condition [40]:

$$G^{-1}(0, 0) = 0 \quad \text{or} \quad \Sigma(0, 0) = \mu. \quad (34)$$

At that point,

$$G^{-1}(k, z_\nu) = z_\nu - \varepsilon_k^0 - [\Sigma(k, z_\nu) - \Sigma(0, 0)]. \quad (35)$$

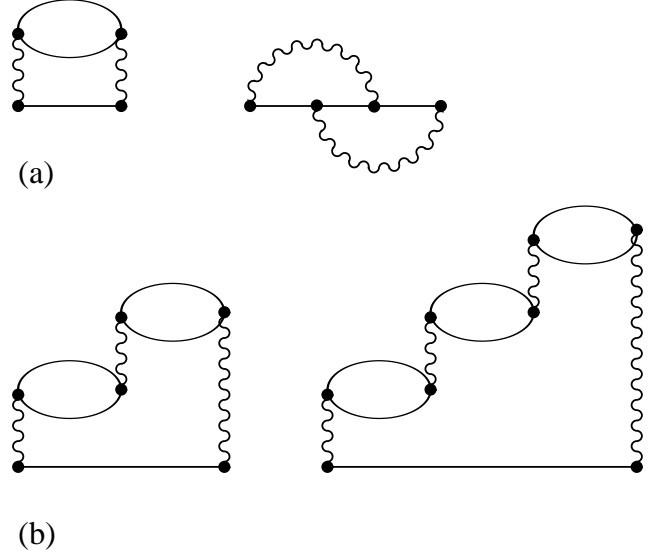


Fig. 4. (a) Green's function diagrams leading to equation (36), similar to Figure 3c. (b) Green's function bubble diagrams leading to equation (97), similar to Figure 3d.

To first order in the interaction strength, the self-energy is given by the Hartree-Fock approximation⁷, leading to a contribution Σ_{HF} (see Eq. (10)) independent of both k and z which can then be eliminated by a redefinition of the chemical potential, as discussed above.

The structure of $\Sigma(k, z)$ in next order is described by the two diagrams in Figure 4a. The second is the exchange term of the first, and within the present approximation in which the matrix elements of the interaction do not depend on momenta, the two contributions are equal. Replacing the free propagators by their Hartree-Fock version, we have

$$\Sigma(k, z_\nu) = 2g^2 \int \frac{d^3k'}{(2\pi)^3} \frac{d^3q}{(2\pi)^3} \times \frac{f_{k'}(1+f_{k'+q})(1+f_{k-q}) - (1+f_{k'})f_{k'+q}f_{k-q}}{z_\nu + \mu' + \varepsilon_{k'}^0 - \varepsilon_{k'+q}^0 - \varepsilon_{k-q}^0}. \quad (36)$$

Because the condensation condition (34) involves only the Matsubara frequency $z_\nu = 0$, we concentrate from now on this contribution. Furthermore, as before, we isolate the dominant contribution by expanding the statistical factors, so that $f_k \sim T/\varepsilon_k^0$, and

$$\Sigma(k, 0) - \Sigma(0, 0) \simeq -2g^2 T^2 \int \frac{d^3k'}{(2\pi)^3} \frac{d^3q}{(2\pi)^3} \times \frac{1}{(\varepsilon_{k'}^0 - \mu')(\varepsilon_{k'-q}^0 - \mu')} \left(\frac{1}{\varepsilon_{k-q}^0 - \mu'} - \frac{1}{\varepsilon_q^0 - \mu'} \right). \quad (37)$$

⁷ Implicit in this expression is the summation of two-body collisions *via* the t -matrix, which relates the two-body potential to the scattering length a at low energies. The summation is made with diagrams where the intermediate propagators are free, corresponding to two particles interacting in the vacuum [41].

Replacing the bare energies ε_k^0 by the dressed energies $\varepsilon_k^0 + \Sigma(k, 0)$, observing that $\mu' = \Sigma(0, 0)$ at the transition, and setting

$$\varepsilon_k = \varepsilon_k^0 + \Sigma(k, 0) - \Sigma(0, 0), \quad (38)$$

we recover equation (31). Note that the earlier $\delta\mu_k - \delta\mu_{k=0}$ is simply $\Sigma(k, 0) - \Sigma(0, 0)$.

3.3 Discussion

The change of the critical density is intrinsically related to $\delta\mu_k$ (or equivalently $\Sigma(k, 0)$) by equation (26). In terms of

$$U(k) = 2m [\delta\mu_k - \delta\mu_{k=0}] = 2m [\Sigma(k, 0) - \Sigma(0, 0)], \quad (39)$$

the change of the critical density introduced by the interaction is

$$\Delta n_c = \int \frac{d^3k}{(2\pi)^3} \left\{ \frac{1}{e^{\beta[k^2 + U(k)]/2m} - 1} - \frac{1}{e^{\beta k^2/2m} - 1} \right\} \quad (40)$$

or

$$\Delta n_c \simeq -\frac{2}{\pi\lambda^2} \int_0^\infty dk \frac{U(k)}{k^2 + U(k)}, \quad (41)$$

where in the second line we have used the approximation (14).

The heart of the calculation of the critical density is then to determine the function $U(k)$, a non-trivial task, since the evaluation of this function by naive perturbation expansion fails because of infrared divergences. However, higher order iterations lead to an instability in the energy spectrum at small momenta, as in reference [21]. In the limit of an infinite number of iterations, the spectrum around $k = 0$ hardens: the self-consistent solution of (24) leads indeed to $\varepsilon_k \sim k^{3/2}$, as predicted by Patashinskii and Pokrovskii [42] using the following argument.

For free particles, the integral in equation (37) contains six powers of momentum in both the numerator and denominator, and is thus logarithmically divergent. In order to ensure that the self-consistent solution, ε_k , converges in the infrared limit, ε_k must behave (modulo possible logarithmic corrections) as $\sim k^\alpha$ with $\alpha < 2$, so that the free particle energies, $\varepsilon_k^0 \sim k^2$, can be neglected at small k with respect to $\Sigma(k, 0) - \Sigma(0, 0)$. With this behavior, $\Sigma(k, 0) - \Sigma(0, 0) \sim k^{6-3\alpha}$, so that we find a self-consistent energy spectrum, $\varepsilon_k \sim \Sigma(k, 0) - \Sigma(0, 0) \sim k^\alpha$, for $\alpha = 3/2$.

The modification of the spectrum occurs only for small momenta $k \ll k_c$, where k_c is a scale that will be specified below. We note here only that since $U(k)$ is of order a^2/λ^4 , one expects k_c to be of order a/λ^2 . For momenta $k_c \ll k \rightarrow \infty$, perturbation theory becomes applicable leading to $U(k)/k^2 \rightarrow 0$. The typical momenta involved in the integral (41) are of order k_c . The validity of equation (41) for $k \ll \lambda^{-1}$ requires $k_c \ll \lambda^{-1}$, which is satisfied in the dilute limit.

We later present numerical self-consistent solutions of equation (31). Here we reconsider the simple analytical

model calculation of reference [16] which provides an estimate for the scale k_c , and acts as a reference for the numerical results presented later. In this analytical model we construct a self-consistent energy spectrum at the critical point:

$$\varepsilon_k = \frac{\hbar^2 k^2}{2m} + \Sigma(k, 0) - \Sigma(0, 0) \quad (42)$$

within the approximation (37) for the self-energy, which we write as

$$\Sigma(k, 0) - \Sigma(0, 0) = -2g^2 T \int \frac{d^3q}{(2\pi)^3} B(q) \left(\frac{1}{\varepsilon_{k-q}} - \frac{1}{\varepsilon_q} \right), \quad (43)$$

where the bubble diagram contributes

$$B(q) = T \int \frac{d^3p}{(2\pi)^3} \frac{1}{\varepsilon_p \varepsilon_{p+q}}. \quad (44)$$

To extract the low momentum structure, below the scale k_c , we evaluate the most divergent terms of equation (43) using the following ansatz:

$$\varepsilon_k = k_c^{1/2} \frac{\hbar^2 k^{3/2}}{2m} \Theta(k_c - k) + \frac{\hbar^2 k^2}{2m} \Theta(k - k_c). \quad (45)$$

With this spectrum, equation (44) becomes

$$B(q) \simeq \frac{4m}{\pi \hbar^2 \lambda^2 k_c} \left[\ln \left(\frac{k_c}{q} \right) + c \right], \quad (46)$$

where $c \approx 2 + 2 \ln 2 - \pi/2 = 1.816$, and in the limit $k \rightarrow 0$ the self-energy is

$$\Sigma(k, 0) - \Sigma(0, 0) = \frac{1024\pi\hbar^2}{15m} \left(\frac{a}{\lambda^2} \right)^2 \left(\frac{k}{k_c} \right)^{3/2}. \quad (47)$$

Identifying the right side of this equation with $k_c^{1/2} \hbar^2 k^{3/2}/2m$, the self-consistency condition, equation (45), in the limit $k \rightarrow 0$ implies that

$$k_c = 32 \left(\frac{2\pi}{15} \right)^{1/2} \frac{a}{\lambda^2} \approx 20.7 \frac{a}{\lambda^2}. \quad (48)$$

As expected, the scale of the low momentum structure is a/λ^2 . However, one should note that the large value of the numerical factor implies that the range of validity of the calculation is limited to very small values of a/λ (so that the condition $k_c \ll \lambda^{-1}$ is fulfilled).

The energy spectrum obtained with this analytical model is only self-consistent for wavevectors $k \ll k_c$. In the limit $k \gg k_c$ we assume that ε_k goes over to the free particle spectrum $\varepsilon_k \simeq \hbar^2 k^2/2m$, ignoring here a logarithmic correction (see Sect. 5). We smoothly interpolate between these limits, writing

$$U(k) = \frac{2m}{\hbar^2} (\Sigma(k, 0) - \Sigma(0, 0)) = \frac{k_c^{1/2} k^{3/2}}{1 + (k/k_c)^{3/2}}. \quad (49)$$

Thus we estimate the critical temperature as

$$\frac{\Delta T_c}{T_c} = \frac{4\lambda}{3\pi\zeta(3/2)} \int_0^\infty \frac{U(k)}{k^2 + U(k)} \simeq 3an^{1/3}. \quad (50)$$

While the precise coefficient is sensitive to the details of the interpolation between the low and high k limits, *e.g.*, (49), the result remains of order unity in any case.

The $k^{3/2}$ spectrum is only an approximation and is not stable if higher order corrections are included; from the general theory of phase transitions, at T_c , $\varepsilon_k \sim k^{2-\eta}$, where $\eta = \varepsilon^2/54 \simeq 0.02$ in an $\varepsilon = 4 - D$ expansion or $\eta = 8/(3\pi^2 N) \simeq 0.14$ in the large N limit (with $N = 2$) [43]. This model provides too strong a modification of the spectrum at small momenta.

The model calculation illustrates however the basic mechanism behind the change of the degeneracy parameter, the modification of the single particle energy spectrum at small momentum. This may be understood as a result of correlations among particles caused by their repulsive interactions: particles minimize their repulsion by avoiding each other in space, *i.e.*, by correlating their positions; the physical origin of the effect is therefore a spatial rearrangement that affects the atoms with low momentum. By contrast, atoms with high momenta have too much kinetic energy to develop significant correlations. The modification of the spectrum translates into a modification of the population of the various levels. In particular the low momentum levels at momentum scale $\sim k_c$ are less populated than they would in a mean field approximation at the same density, and the overall result is a decrease of the critical density.

The hardening of the spectrum obtained as a solution of the self-consistent equations, which is responsible for the decrease of the critical density, also provides a cure for the infrared divergences which occur in the perturbative calculation in second order. However, as we shall see in the next section, such divergences appear in all orders in perturbation theory, so that we need a more general scheme to approach the problem.

4 Classical field approximation

In this section we extend the discussion of the previous section in a way that is at the same time more general, in that it is not restricted to any particular class of diagrams, and less general, in that only the linear corrections to the density are investigated.

4.1 Breakdown of perturbation theory

Our main goal is the calculation of the critical density. As an intermediate step, we distinguish in equation (33) for ρ_k the contribution of zero and non-zero Matsubara frequencies:

$$\rho_k = -TG(k, 0) - T \sum_{\nu \neq 0} G(k, i\omega_\nu). \quad (51)$$

The density is obtained by integrating over momentum k (see Eq. (18)). The terms with $\nu \neq 0$ are regular at small momentum since a non-vanishing Matsubara frequency provides an infrared cutoff. They provide corrections to the density, that are analytic in the self-energy, and therefore of the same order as Σ , starting at order a^2 (modulo possible logarithmic corrections). On the other hand, the integral for $\nu = 0$ is singular for small k , and the infrared divergences introduce non-analyticity in a . Since, we are interested here in the dominant correction to the critical density, we will retain only this term in ρ_k . Note that the resulting expression for the density is ultraviolet divergent, a problem bypassed by calculating the change in the critical density.

As illustrated by the example of the previous section, infrared divergences also occur in the calculation of self-energies $\Sigma(k, 0)$; we now use simple power counting arguments to analyze these divergences. Let us first consider diagrams in which all the internal lines carry zero Matsubara frequencies. It is convenient here to introduce a new notation and set

$$\varepsilon_k^0 - \mu' = (k^2 + \zeta^{-2})/2m. \quad (52)$$

The quantity ζ , a the mean field correlation length, is given by

$$\frac{\hbar^2}{2m\zeta^2} = -\mu' = -(\mu - \Sigma_{\text{HF}}); \quad (53)$$

ζ plays the role of an infrared cutoff in the integrals. Note that $\zeta \rightarrow \infty$ ($\mu' \rightarrow 0$) when $T \rightarrow T_c^0$. In the perturbation series, we take the intermediate propagators to be neither free, nor fully self-consistent as in the previous section, but containing the mean field contributions. All the functions that are integrated in the diagrams then appear as products of fractions of the form

$$[K^2 + \zeta^{-2}]^{-1}, \quad (54)$$

where K denotes a generic combination of momenta; it is then natural to use the dimensionless products $K\zeta$ as new integration variables. Consider then a diagram of order a^n . The lowest order $n = 2$ has been already explicitly written in (37), and it is proportional to $(a/\lambda)^2 \ln(k\zeta)$, where k is the external momentum. For $n > 2$, every additional order brings in one factor a from the vertex, one integration over three-momenta, a factor T , and two Green's functions (the internal lines). The contribution of the diagram can thus be written as:

$$T \left(\frac{a}{\lambda}\right)^2 \left(\frac{a\zeta}{\lambda^2}\right)^{n-2} F(k\zeta), \quad (55)$$

where F is a dimensionless function, which we do not explicitly need here. The main point is that when one approaches the critical temperature, the coherence length becomes large so that the summation of terms (55) diverges. In the critical region, ζ is $\sim \lambda^2/a$, so that all the terms in the perturbative expansion are of the same order

of magnitude. Therefore, at the critical point, perturbation theory is not valid.

Let us now assume that in a given diagram some propagators carry non-zero Matsubara frequencies so that one momentum integration will be altered. For that integration, the presence of an additional imaginary term $2i\pi\nu T$ in the denominators of the propagators ensures that no singularity at $k = 0$ can take place. Essentially, in the corresponding propagators, ζ is replaced by a term proportional to λ , so that one factor $a\zeta/\lambda^2$ in (55) is now replaced by a/λ . Compared to the diagram with only vanishing Matsubara frequencies, this diagram is down by a factor a/λ , and thus negligible in a leading order calculation of Σ .

4.2 Classical field approximation

The diagrams where all Matsubara frequencies vanish are those of an effective theory for static fields. Ignoring the non-zero Matsubara frequencies is indeed equivalent to ignoring the (imaginary) time dependence of the field operators. In this approximation the many-body problem reduces to a classical field theory in three space dimensions.

The energy of a classical field configuration is given by

$$\mathcal{H} = \int d^3r \left(\frac{|\nabla\varphi(r)|^2}{2m} - \mu'|\varphi(r)|^2 + \frac{2\pi a}{m}|\varphi(r)|^4 \right). \quad (56)$$

The zero Matsubara component of the density is given by $\langle |\varphi(r)|^2 \rangle$. By assumption, the wavenumbers of the classical field are limited to k less than an ultraviolet cutoff $\Lambda \sim \lambda^{-1}$. As one approaches the critical region, $k \lesssim k_c$, all the terms in the integrand of (56) become of the same order of magnitude:

$$\frac{k_c^2}{2m} \sim \mu' \sim \frac{a}{m} \frac{T}{\mu'} k_c^3, \quad (57)$$

where $(T/\mu')k_c^3$ is the contribution to the density of the modes with $k \sim k_c$. From equation (57) we see that $k_c \sim a/\lambda^2$. For $k \simeq k_c$ perturbation theory in a makes no sense, and in fact all terms in the perturbative expansion are infrared divergent. For $k_c \ll k \ll \lambda^{-1}$, perturbation theory is applicable. Note that, in the critical region, $\zeta \sim 1/k_c \sim \lambda^2/a$.

By a simple rescaling of the fields $\varphi \rightarrow \sqrt{mT}\phi$, one can write the effective action for the classical field theory as

$$-\mathcal{H}/T = \int d^3r \left(\frac{1}{2}|\nabla\phi(r)|^2 - m\mu'|\phi(r)|^2 + \frac{4\pi^2 a}{\lambda^2}|\phi(r)|^4 \right). \quad (58)$$

The rescaled fields ϕ have the dimensions of an inverse length. The classical theory contains ultraviolet divergences, which spoil simple dimensional arguments for the linear change of T_c .

4.3 Linear dependence of the density correction

We now consider a diagrammatic expansion of Σ in terms of the full zero frequency Green's function, defined by:

$$-2mG^{-1}(k) = k^2 - 2m\mu + 2m\Sigma(k, a, G, \Lambda), \quad (59)$$

from here on we omit the explicit index $\nu = 0$ in Σ and G . In this self consistent expression the self-energy Σ depends on μ only through its dependence on G . Instead of μ , we use the dimensionless parameter α defined by

$$-2m\mu + 2m\Sigma(0) = \alpha \frac{a^2}{\lambda^4}. \quad (60)$$

The parameter α controls the distance to the critical point; it vanishes exactly at the transition, as opposed to μ . In terms of α the Green's function is now given by:

$$-2mG^{-1}(k) = k^2 + \alpha \frac{a^2}{\lambda^4} + U(k), \quad (61)$$

where

$$U(k) = 2m\Sigma(k, a, G, \Lambda) - 2m\Sigma(0, a, G, \Lambda). \quad (62)$$

Since Σ depends only on the full Green's function, $U(k)$ depends only on α and not on $\Sigma(0)$; moreover, the ultraviolet divergence in $\Sigma(k)$ is only logarithmic, and the difference $U(k)$ is independent of the cutoff Λ in the limit $\Lambda \rightarrow \infty$.

If we assume that $\Lambda \rightarrow \infty$, the power counting analysis of Section 4.1 implies that

$$U(k) = \frac{a^2}{\lambda^4} \tilde{\sigma} \left(\frac{k\lambda^2}{a}, \alpha \right). \quad (63)$$

Inserting this result into (41) and making the change of variable $x = k\lambda^2/a$, one finds

$$\Delta n_c = -\frac{2a}{\pi\lambda^4} \lim_{\alpha \rightarrow 0} \int dx \frac{\tilde{\sigma}(x, \alpha)}{x^2 + \tilde{\sigma}(x, \alpha)}, \quad (64)$$

showing that the change in the critical density is indeed linear in a .

This result assumes that the limit $\tilde{\sigma}(x, \alpha \rightarrow 0)$ is well defined. This is the case in the self-consistent schemes that we discussed above; they avoid the infrared problem of perturbative calculations, and lead to well defined values of Δn_c . Similarly, in calculations involving resummations of bubbles or ladder diagrams the cutoff is provided by an effective screening explicitly generated by the infinite resummations. Large N techniques lead to a similar screening, with the advantage of also providing an expansion parameter [22, 44].

On the other hand, situations where the limit $\tilde{\sigma}(x, \alpha \rightarrow 0)$ is problematic are encountered in perturbation theory where, for reasons discussed above, an infrared cutoff is needed; determination of this cutoff through the condensation condition can lead to spurious a dependence (an explicit example is worked out in detail in the next section).

The linearity of the shift in the critical density does not depend on the ultraviolet cutoff and is thus an universal quantity. Nevertheless, the universal behavior implicitly assumes that the limit $\Lambda \rightarrow \infty$ has been taken and is strictly valid only in the limit $a \rightarrow 0$. If a is not sufficiently small, the classical field approximation ceases to be valid and non-linear corrections appear. The classical field approximation requires that all momenta involved in the various integrations are small in comparison with $\Lambda \sim \lambda^{-1}$ or, in other words, that the integrands are negligibly small for momenta $k \sim \lambda^{-1}$. Only then, for instance, can we use the approximate form of the statistical factors (29). This requires in particular that $k \sim k_c \ll \Lambda$, yielding $a/\lambda \ll 1$. In fact, because, as we shall see, the relation between k_c and a/λ involves a large number, this regime is reached only for very small values, $a/\lambda \lesssim 10^{-2} - 10^{-3}$.

5 Explicit calculations

Our goal in this section is to provide specific illustrations of the discussions of the previous sections. We first present analytical calculations which shed light on the difficulties encountered when attempting to calculate the shift in the critical temperature using perturbation theory. Then we show how partial resummations of the perturbative expansion generate screening of long range correlations and allow an explicit calculation of the self-energy, and then of the transition temperature. Finally we present results of numerical self-consistent calculations, which we compare with the analytical counterparts, and evaluate the limitations of the classical field theory. The accuracy of such approximative schemes is difficult to gauge a priori. An alternative is to use lattice calculations to solve the three-dimensional classical field theory. Results of such calculations have been presented recently [23, 24].

5.1 Second order perturbation theory

In order to illustrate the difficulties that one meets in perturbative calculation near T_c , let us return for a moment to the second order self-energy diagram, which is the lowest order diagram that introduces correlations and therefore corrections to the critical density. The value of this diagram for vanishing Matsubara frequencies is given by equation (37)

$$\begin{aligned} \Sigma(k) - \Sigma(0) &= -2g^2 T^2 \int \frac{d^3 k'}{(2\pi)^3} \frac{d^3 q}{(2\pi)^3} \\ &\times \frac{1}{(\varepsilon_{k'}^0 - \mu')(\varepsilon_{k'-q}^0 - \mu')} \left[\frac{1}{\varepsilon_{k+q}^0 - \mu'} - \frac{1}{\varepsilon_q^0 - \mu'} \right], \quad (65) \end{aligned}$$

where $g = 4\pi a/m$.

We note that $\Sigma(k)$ is the convolution of three factors of the form $1/(k^2 + \zeta^{-2})$, with ζ defined in equation (53). Using the Fourier transform

$$\int \frac{d^3 k}{(2\pi)^3} \frac{e^{ikr}}{k^2 + \zeta^{-2}} = \frac{1}{4\pi r} e^{-r/\zeta}, \quad (66)$$

we obtain

$$2m\Sigma(k) = -128\pi^2 \left(\frac{a}{\lambda^2}\right)^2 \int r^2 dr j_0(kr) \left(\frac{e^{-r/\zeta}}{r}\right)^3, \quad (67)$$

where $j_0(x) \equiv \sin x/x$. This expression contains, as anticipated, a logarithmic divergence at small distances. Let us isolate this divergence by separating the Bessel function $j_0(x)$ into its value at the origin and a correction term:

$$j_0(x) = j_0(0) + \left(\frac{\sin x}{x} - 1\right). \quad (68)$$

The first term gives a momentum independent contribution, given by $\Sigma(0)$. Introducing a cutoff $1/\Lambda$ to control the ultraviolet divergence, we obtain

$$\begin{aligned} 2m\Sigma(0) &= 128\pi^2 \left(\frac{a}{\lambda^2}\right)^2 \text{Ei}\left(-\frac{3}{\Lambda\zeta}\right) \\ &\approx -128\pi^2 \left(\frac{a}{\lambda^2}\right)^2 \left[\ln\left(\frac{\Lambda\zeta}{3}\right) - \gamma\right], \quad (69) \end{aligned}$$

where $\gamma = 0.577\dots$ is Euler's constant, and Ei the exponential integral function. The last approximate equality is valid when $\Lambda\zeta \gg 1$, which we assume to be the case. The second term, which is regular and equal to $2m(\Sigma(k) - \Sigma(0)) = U(k)$, does not require a cutoff. The result is

$$\begin{aligned} U(k) &= -128\pi^2 \left(\frac{a}{\lambda^2}\right)^2 \int_0^\infty (j_0(kr) - 1) \frac{e^{-3r/\zeta}}{r} dr \\ &= 128\pi^2 \left(\frac{a}{\lambda^2}\right)^2 \left\{ \frac{3}{k\zeta} \arctan \frac{k\zeta}{3} + \frac{1}{2} \ln \left(1 + \left(\frac{k\zeta}{3}\right)^2 \right) - 1 \right\}. \quad (70) \end{aligned}$$

This equation implies that $U(k)$ is a monotonically increasing function of k , $\sim k^2$ at small k , and growing logarithmically at large k . This logarithmic behavior, obtained in perturbation theory, remains in general the dominant behavior of $U(k)$ at large k , *i.e.*, for $\zeta^{-1} \ll k \lesssim \Lambda$.

Our result for $U(k)$ can now be used in equation (41) in order to determine the change in the critical density from equation (41). Because $U(k) > 0$, this change is negative. We get:

$$\begin{aligned} \Delta n_c &= -\frac{2}{\pi\lambda^2} \int_0^\infty dk \frac{U(k)}{k^2 + U(k)} \\ &= -\frac{2}{\pi\lambda^2} k_c \int_0^\infty dx \frac{J\sigma(x)}{x^2 + J^2\sigma(x)}, \quad (71) \end{aligned}$$

where we have set

$$x = k\zeta \quad k_c = 8\pi^2 \frac{a}{\lambda^2}, \quad U(k) \equiv k_c^2 \sigma(x), \quad J = \zeta k_c. \quad (72)$$

Note that for small x , $\sigma(x) \sim x^2/27\pi^2$ while at large x , $\sigma(x) \sim 2(\ln(x/3) - 1)/\pi^2$. The function

$\sigma(x)/x^2 \propto \Delta\varepsilon_k/\varepsilon_k$ gives an indication, independent of the specific values of the parameters, of the range of values of x over which the single particle spectrum is significantly modified, and hence of the range of momenta contributing to Δn_c : this function monotonically decreases with x , reaching half its maximum value for $x \approx 7$, and about 1/10 of its maximum when $x \approx 20 - 30$. Comparison of this momentum scale with the characteristic momentum scale of higher Matsubara frequencies ($1/\lambda \sim 1/\Lambda$) gives a constraint on the values of a for which the calculation is meaningful. In particular, a has to be small enough that $a/\lambda \ll \frac{1}{30}(J/8\pi^2)$.

As noted earlier, the momentum dependence of $\Sigma(k)$ is essential for Δn_c to be non-vanishing. In this second order calculation, the (statistical quasiparticle) spectrum remains quadratic at small k , and is given by

$$\epsilon_k \rightarrow \frac{k^2}{2m} \left(1 + \frac{J^2}{27\pi^2} \right), \quad \text{for } k \rightarrow 0. \quad (73)$$

As expected, the spectrum of the interacting system is harder than the free spectrum. In the present approximation, it is identical to the spectrum of non-interacting particles with an effective mass $m^* < m$.

The final result for Δn_c depends on the infrared cutoff ζ , which can be determined by the condensation condition $\mu' = \Sigma(0)$:

$$\frac{1}{\zeta^2} = \frac{2}{\pi^2} k_c^2 \left[\ln \left(\frac{\Lambda\zeta}{3} \right) - \gamma \right]. \quad (74)$$

In principle the ultraviolet cutoff Λ could be eliminated by an appropriate counterterm calculable in the full theory. Alternatively, one could calculate $\Sigma(0)$ from the expression (36) involving the complete statistical factors. The result of such a calculation would be to replace the term $\ln(\Lambda\zeta)$ in equation (69) by $\ln(\zeta/\lambda)$, up to a numerical additive constant. Here we shall simply choose an ultraviolet cutoff $\Lambda = 1/\lambda$, keeping in mind that there is arbitrariness in the procedure which affects the final result, since for $a/\lambda \ll 1$, then $\zeta \gg \lambda$, and $\ln(\zeta/\lambda)$ will eventually dominate. Nevertheless, it is instructive to solve the equation above for ζ as a function of a with this choice of cutoff. Typical values are given in the table below:

a/λ	ζ/λ	J	c
0.01	6.5	5.1	2.4
0.001	23	1.8	0.90
10^{-4}	153	1.2	0.60
10^{-5}	1208	0.95	0.47
...
10^{-9}	7.510^6	0.59	0.29
10^{-10}	7.010^7	0.55	0.27
10^{-11}	6.510^8	0.51	0.25

The behavior of ζ with a is understandable: if a is large, condensation takes place far from the mean field value, hence the small ζ . If a is small, condensation takes place

near the mean field value for which $\zeta \rightarrow \infty$. In fact equation (74) shows that $\zeta \sim \lambda^2/a$ up to a logarithmic correction. The last column of the table gives the coefficient c in equation (4) for ΔT_c . The variation of ΔT_c with a follows closely that of $J \int dx \sigma(x)/x^2 = J/6\pi$; that is, the term in J^2 in the denominator plays almost no role⁸.

This simple calculation also illustrates the limits of a perturbative approach. The infrared cutoff introduces a new scale in the problem which spoils the argument leading to the linearity of the a -dependence of ΔT_c (c is not a constant). The condensation condition (74) which relates the infrared cutoff to the microscopic length λ , induces a spurious logarithmic correction which does not vanish as $a \rightarrow 0$.

5.2 Non self-consistent bubble sums

The previous calculation illustrates how the mixing of ultraviolet and infrared divergences in perturbation theory can produce spurious a dependences. It is therefore desirable to find approximations in which the infrared cutoff is internally generated. One such approximation was already presented in Section 3.3. We turn now to another, the resummation of bubble diagrams, as illustrated in Figure 4b. Again, the quality of such an approximation can only be gauged by a comparison with an exact calculation, except in large N limit where the bubble summation becomes exact itself [22, 44].

The one bubble diagram can be calculated explicitly. Keeping an infrared cutoff, we have

$$\begin{aligned} B(q) &= T \int \frac{d^3p}{(2\pi)^3} \frac{1}{(\varepsilon_p^0 - 1/2m\zeta^2)(\varepsilon_{p+q}^0 - 1/2m\zeta^2)} \\ &= \frac{4\pi}{\lambda^4 T q} \arctan \frac{q\zeta}{2}. \end{aligned} \quad (75)$$

In the infinite cutoff limit ($\zeta \rightarrow \infty$) this simplifies into

$$B(q) = \frac{2\pi^2}{\lambda^4 T} \frac{1}{q}. \quad (76)$$

The Fourier transform of $B(q)$ is nothing but the leading contribution to the density-density correlation function. At the critical point this correlations behaves as $1/r^2$, so that density fluctuations are correlated over very large distances; this is the physical origin of the infrared divergences of perturbative calculations. Nevertheless, these fluctuations can be screened, for instance by summing the bubble or ladder diagrams. The respective contributions of the two classes of diagrams actually differ only by the number of exchange diagrams. For the bubble sum, the correlation function reads

$$\frac{B(q)}{1 + 2gB(q)} = \frac{2\pi^2}{\lambda^4 T} \frac{1}{q + k_c}, \quad (77)$$

⁸ Note that these second order results are closely related to the perturbative calculation of [21] where $c \sim 1$ was obtained by looking at values $0.001 \leq a/\lambda \leq 0.01$.

and is now regular at small q . The screening wave number k_c is given by

$$k_c = 8\pi^2 \frac{a}{\lambda^2}. \quad (78)$$

In the ladder approximation the factor of 2 in the denominator of (77) is absent, and, correspondingly, $k_c = 4\pi^2 a/\lambda^2$.

Now, an infrared cutoff is no longer needed in the calculation of $U(k)$, and the limit $\zeta \rightarrow \infty$ can be taken. One finds

$$U(k) = -\frac{2}{\pi^2} k_c^2 \kappa \int_0^\infty dx \frac{1}{1+x\kappa} \left[\frac{x}{2} \ln \left| \frac{1+x}{1-x} \right| - 1 \right], \quad (79)$$

where $\kappa \equiv k/k_c$. To study the limiting behavior of $U(k)$ at large and small k , it is convenient to transform this expression as follows. First we integrate twice by parts to obtain

$$U(k) = -\frac{2}{\pi^2} \frac{k_c^2}{\kappa} \int_0^\infty dx \frac{2(1+x\kappa)[\ln(1+x\kappa) - 1]}{(1-x^2)^2}. \quad (80)$$

Taking the derivative of the integrand with respect to κ which obtain

$$\begin{aligned} \frac{d}{d\kappa} \int_0^\infty dx \frac{2(1+x\kappa)[\ln(1+x\kappa) - 1]}{(1-x^2)^2} &= \frac{1}{2} \int dx \ln(1+x\kappa) \\ &\times \left(\frac{1}{(1-x)^2} - \frac{1}{(1+x)^2} \right) = \frac{\kappa^2}{1-\kappa^2} \ln \kappa. \end{aligned} \quad (81)$$

The κ integral can now be expressed in terms of the polylogarithmic function $g_p(x)$, defined in equation (7); the integration constant is chosen to make $U(k=0) = 0$. Thus,

$$U(k) = -\frac{2}{\pi^2} \frac{k_c^2}{\kappa} \left\{ \kappa[1 - \ln \kappa] + \frac{1}{2} \ln \kappa \ln(1 + \kappa) + \frac{1}{2} [g_2(1 - \kappa) + g_2(-\kappa)] - \frac{\pi^2}{12} \right\}. \quad (82)$$

However, to derive the limiting behavior of $U(k)$ it is more convenient to take the limits in equation (81) and integrate afterwards.

For small κ ($\kappa = k/k_c \lesssim 0.1$), $U(k)$ is well approximated by its small k behavior:

$$U(k) = -\frac{2}{3\pi^2} k^2 \left(\ln \frac{k}{k_c} - \frac{1}{3} \right), \quad k \ll k_c. \quad (83)$$

As expected from perturbation theory, $U(k)$ grows logarithmically for large momenta, k , and for $k/k_c \gtrsim 50$, $U(k)$ is well approximated by:

$$U(k) = \frac{2k_c^2}{\pi^2} \left(\ln \frac{k}{k_c} - 1 \right), \quad k/k_c \gg 1. \quad (84)$$

From the small k behavior of $k^2 + U(k)$ one can estimate the critical index η . The logarithmic term indicates a modified power law in the low momentum

limit $\sim k^{2-\eta} \sim k^2(1 - \eta \ln k + \dots)$. Comparing the coefficients of the logarithmic terms we obtain

$$\eta = \frac{2}{3\pi^2} \approx 0.068. \quad (85)$$

Due to the exchange contributions this value differs by a factor of 2 from the usual large N results⁹.

The change in the critical density is now

$$\Delta n_c = -\frac{2k_c}{\pi\lambda^2} \int_0^\infty d\kappa \frac{\sigma(\kappa)}{\kappa^2 + \sigma(\kappa)}. \quad (86)$$

Let us first estimate the range of $\kappa_0 = k_0/k_c$ where $\sigma(\kappa)$ dominates over κ^2 . Using the small k asymptotics of $U(k)$ we estimate $\kappa_0 \lesssim \exp[-3\pi^2/2] \ll 1$. Therefore, we can again ignore the term in $\sigma(\kappa)$ in the denominator of (86) without making a significant error; it only brings in an harmless singularity at small κ . We get then:

$$\frac{\Delta n_c}{n_c} = \frac{4k_c\lambda}{\pi^3\zeta(3/2)} \int_0^\infty \frac{d\kappa}{\kappa} \int_0^\infty \frac{dx}{1+x\kappa} \left(\frac{x}{2} \ln \left| \frac{1+x}{1-x} \right| - 1 \right). \quad (87)$$

In order to calculate the integral, we want to exchange the orders of the κ and x integrals. Since the integrals, however, are not absolutely convergent, before we do so we need to introduce a regularization, inserting a factor κ^ϵ in the κ integral, and taking the limit $\epsilon \rightarrow 0^+$. With this factor we may exchange the orders of integration. The κ integral becomes

$$\int_0^\infty d\kappa \frac{\kappa^{\epsilon-1}}{1+x\kappa} = \frac{1}{\epsilon x^\epsilon}. \quad (88)$$

The remaining x integral becomes

$$\int dx x^{-\epsilon} \left(\frac{x}{2} \ln \left| \frac{1+x}{1-x} \right| - 1 \right). \quad (89)$$

For $\epsilon = 0$ this integral vanishes identically. Thus we may replace $x^{-\epsilon}$ by $x^{-\epsilon} - 1$ which goes to $-\epsilon \ln x$ as $\epsilon \rightarrow 0$. The remaining integral is

$$\int dx \ln x \left(\frac{x}{2} \ln \left| \frac{1+x}{1-x} \right| - 1 \right) = -\frac{\pi^2}{8}. \quad (90)$$

⁹ Note however that the expansion in powers of η is meaningful only if the magnitude of η is controlled by a small parameter, such as in the ϵ -expansion or the $1/N$ -expansion. The estimate presented here should therefore not be viewed as a particular prediction for the critical index η ; it gives nevertheless an indication of how the spectrum is modified at small k by the resummation of particle-hole bubbles. Another estimate of the effect of bubble summation was presented in reference [16]; there we tried to estimate the change of the spectrum with respect to the $k^{3/2}$ self-consistent solution. Once the bubble sum is included however, self-consistency does not further alter the spectrum at low momentum, as later in this section. As a result, the exponent η that one finds here is much smaller than the crude estimate in reference [16].

The factors of ϵ cancel out, and we find

$$\frac{\Delta n_c}{n_c} = -\frac{k_c \lambda}{2\pi \zeta(3/2)} = -\frac{4\pi}{\zeta(3/2)} \frac{a}{\lambda}. \quad (91)$$

We finally obtain the changes in the transition density and the transition temperature:

$$\begin{aligned} \frac{\Delta n_c}{n_c} &= -\frac{4\pi}{\zeta(3/2)^{4/3}} a n^{1/3} \\ \frac{\Delta T_c}{T_c} &= -\frac{2}{3} \frac{\Delta n_c}{n_c} \simeq 2.33 a n^{1/3}, \end{aligned} \quad (92)$$

this result for the bubble sum agrees with the leading order result of the $1/N$ expansion. It is interesting to observe that the leading order $1/N$ result is independent of N . Since aN is kept constant in the $1/N$ expansion, k_c is effectively independent of N ($k_c = 2\pi^2 a N / \lambda^2$), while $U(k)$ is of order $1/N$. Therefore, the approximation of neglecting $U(k)$ in the denominator of equation (86) is justified in the $1/N$ expansion.

In the bubble sum, we can keep $U(k)$ in the denominator and calculate the integral in equation (86) numerically, and find a reduction the linear coefficient of the critical temperature shift from $c = 2.33$ to $c = 2.20$ for $N = 2$. In this approximation the condensation condition reads

$$2m\Sigma(0) = -\frac{2k_c^2}{\pi^2} \int_0^{\Lambda/k_c} dx \frac{1}{1+x^2} = \frac{2k_c^2}{\pi^2} \ln \frac{k_c}{\Lambda + k_c}, \quad (93)$$

which gives the mean field correlation length,

$$\frac{1}{\zeta^2} = \frac{2k_c^2}{\pi^2} \ln \frac{1}{\lambda k_c}. \quad (94)$$

As before we have taken $\Lambda = 1/\lambda$ and assumed that $\lambda k_c \ll 1$. As opposed to the second order calculation, equation (74), the condition (93) does not mix the infrared and ultraviolet cutoff, and does not introduce any spurious a dependence in the final result for the shift in the critical temperature.

The condensation condition (93) is the only place where the microscopic scale λ enters explicitly. However, the classical field theory result for ΔT_c assumes implicitly that the contributions of momenta $k \sim \lambda^{-1}$ are vanishingly small. Alternatively, if we were to cut the integration in (86) off at $k \sim \Lambda$, one should find a result independent of the specific value of $\Lambda \gtrsim \lambda^{-1}$. In fact we have seen that the momenta important in the determination of ΔT_c are $k \sim k_c$. The validity of the classical field approximation requires that $k_c \ll \lambda^{-1}$, or, since $k_c = 8\pi^2 a \lambda^2$, $a/\lambda \ll 1/8\pi^2$; thus, the linear regime is attained only for anomalously small a . When a is not so small, non-linear corrections $\sim a^2 \ln(a/\lambda)$ appear, which tend to decrease the value of ΔT_c , as discussed in reference [18] (see also below).

In reference [14], Stoof examines the appearance of Bose-Einstein condensation, calculating the shift of the critical density within a real time formalism. The approach includes not only the mean field contributions

but also sums of ladder graphs within the many-body T -matrix-approximation. He derives an analytical formula for the modification of the energy spectrum, from which he derives a relative increase of the critical temperature, $4.66 a n^{1/3}$, exactly twice the value of the large- N calculation [22]. Summing ladders, and neglecting $U(k)$ in the denominator of equation (86) we indeed reproduce this result. Evaluating the entire integral numerically, one obtains $c = 3.90$.

5.3 Self-consistent calculations

We now solve numerically the self-consistent calculations discussed in Section 3.3. We quantitatively compare three different approximations for the self-energy, the one bubble approximation, equation (43),

$$\Sigma(k) - \Sigma(0) = -2g^2 T \int \frac{d^3 q}{(2\pi)^3} B(q) \left(\frac{1}{\epsilon_{k-q}} - \frac{1}{\epsilon_q} \right), \quad (95)$$

and, to compare with previous calculations, the ladder summation of particle-particle scattering processes

$$\Sigma(k) - \Sigma(0) = -2g^2 T \int \frac{d^3 q}{(2\pi)^3} \frac{B(q)}{1 + gB(q)} \left(\frac{1}{\epsilon_{k-q}} - \frac{1}{\epsilon_q} \right). \quad (96)$$

And, finally, the bubble summation of particle-hole scattering processes

$$\Sigma(k) - \Sigma(0) = -2g^2 T \int \frac{d^3 q}{(2\pi)^3} \frac{B(q)}{1 + 2gB(q)} \left(\frac{1}{\epsilon_{k-q}} - \frac{1}{\epsilon_q} \right), \quad (97)$$

the energy spectrum ϵ_k in the denominators are determined self-consistently using equation (42); $B(q)$ is given in equation (44).

Although the integrals in equations (95–96) giving the difference of the self-energies, $U(k) = 2m[\Sigma(k) - \Sigma(0)]$, are convergent, we introduce a large momentum cutoff Λ for their numerical evaluation ($U(k \geq \Lambda) \equiv 0$). Only in the limiting case $\Lambda \rightarrow \infty$, will $U(k)$ become independent of Λ ; for any finite cutoff, the energy spectrum depends weakly on Λ . The cutoff enters only through the dimensionless parameter $\Lambda \lambda^2 / a$. For the numerical calculation the value $\Lambda \lambda^2 / a \simeq 800$ was used. For the self-consistent bubble calculation we further studied the influence of the cutoff to extrapolate numerically to the limit $\Lambda \rightarrow \infty$.

Figure 5 summarizes the numerical results of this section in terms of the self-energies $\Sigma(k) - \Sigma(0)$ corresponding to the three different approximations. The various curves in Figure 5 display the logarithmic growth of $U(k)$ at large k . Note however that within the present approximations the overall magnitude of $U(k)$ is determined by the behavior of the spectrum at small k : the harder the spectrum, the larger $U(k)$, and the larger the value of c . Nevertheless, the values of the shifts in the critical temperature remain comparable. For instance, for the

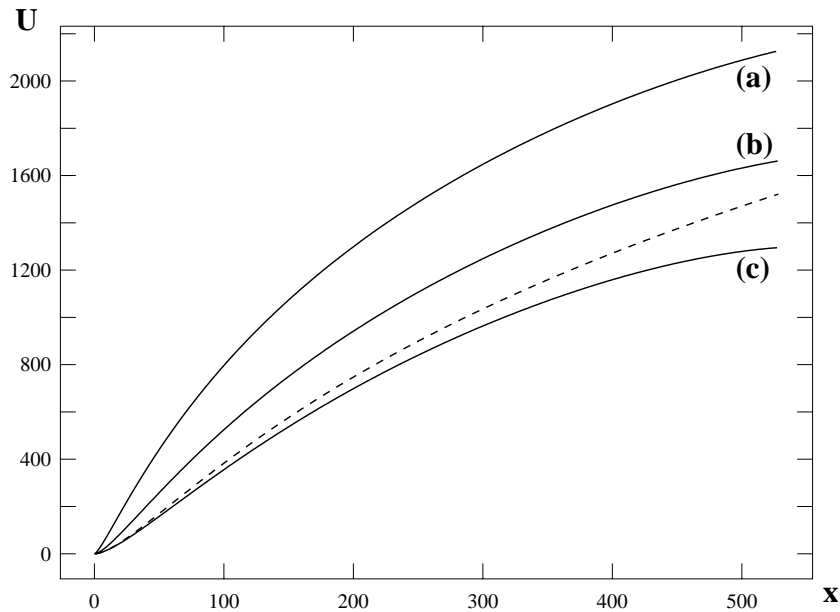


Fig. 5. Self-energy $U(k)$ in units of a^2/λ^4 plotted as a function of $x = k^2/a$ for the three approximations discussed in the text: (a) self-consistent one bubble approximation, (b) self-consistent ladder summation, and (c) self-consistent bubble sum. These results are obtained with an ultraviolet cutoff of $\Lambda\lambda^2/a \simeq 800$. The dashed line shows the analytical (not self-consistent) calculation of $U(k)$ in the bubble approximation, equation (82).

value of the cutoff given above, the shifts of the critical temperature that we obtain from equation (41) are: $\Delta T_c/T_c^0 \simeq 3.8 an^{1/3}$ for the self-consistent one bubble calculation, $\Delta T_c/T_c^0 \simeq 1.6 an^{1/3}$ for the self-consistent bubble sum, and $\Delta T_c/T_c^0 \simeq 2.5 an^{1/3}$ for the self-consistent ladder sum. These values still depend weakly on the value of the ultraviolet cutoff Λ , and still contain logarithmic corrections $\sim a^2 \ln(a/\lambda)$, as we shall see below.

We now compare in more detail these results with our analytical calculations and discuss briefly the extrapolation $\Lambda \rightarrow \infty$, *i.e.* the extrapolated result of the bubble summation is $\Delta T_c/T_c \simeq 2.0 an^{1/3}$.

5.3.1 Self-consistent one-bubble calculation

In the limit $k \rightarrow 0$, we expect to recover the $k^{3/2}$ behavior of the analytical model of Section 3.3. By fitting the numerical data to the following functional form

$$2m(\Sigma(k) - \Sigma(0)) = \frac{k_c^{1/2} k^{3/2}}{1 + a_{1/2}(k/k_c)^{1/2} + a_1(k/k_c) + a_{3/2}(k/k_c)^{3/2} + \dots}, \quad (98)$$

we extract a momentum scale k_c , which agrees quantitatively with that of the analytical calculation, $k_c \sim 20 a/\lambda^2$. However, the spectrum very soon deviates from this behavior, due to the large value of the coefficient $a_{1/2} \simeq 0.9$. At intermediate wavevectors, around k_c , $U(k)$ is roughly linear, and eventually grows logarithmically for $k \gg k_c$, as expected from perturbation theory.

5.3.2 Self-consistent bubble sum

As we have seen in a previous example the main effect of self-consistency is to modify the spectrum at low momentum, avoiding infrared divergencies. Since, however, the bubble sum already provides a screening of the long range correlations leading to the infrared divergences, we do not expect qualitative changes in $U(k)$ in going from the non self-consistent result of Section 5.2, to the fully self-consistent calculations. This behavior can be seen in Figure 5: deviations occur only at high momenta, mainly due to the influence of the finite cutoff in the numerical solution.

To study more quantitatively the influence of a large but finite cutoff Λ we have performed a self-consistent calculation of $U(k)$ numerically for several values of $\Lambda\lambda^2/a$. As explained in reference [18] we expect a logarithmic dependence on $\Lambda\lambda^2/a$; therefore we have used this functional form to fit our numerical data, which provides

$$\frac{\Delta T_c}{T_c} \simeq 1.95 an^{1/3} \left[1 + 32 \frac{an^{1/3}}{\Lambda\lambda} \ln \left(21 \frac{an^{1/3}}{\Lambda\lambda} \right) \right], \quad \Lambda/a \gg 1. \quad (99)$$

Extrapolating to $\Lambda \rightarrow \infty$ we obtain $c \simeq 2.0$, which is slightly smaller than the shift obtained for the non self-consistent bubble sum. Alternatively, taking a finite value for $\Lambda\lambda$ that is independent of a , *e.g.* $\Lambda\lambda \sim 1$, provides a logarithmic correction which limits the linear regime to very small values of $an^{1/3}$. The precise value of this correction is model dependent, as we see in the following subsection.

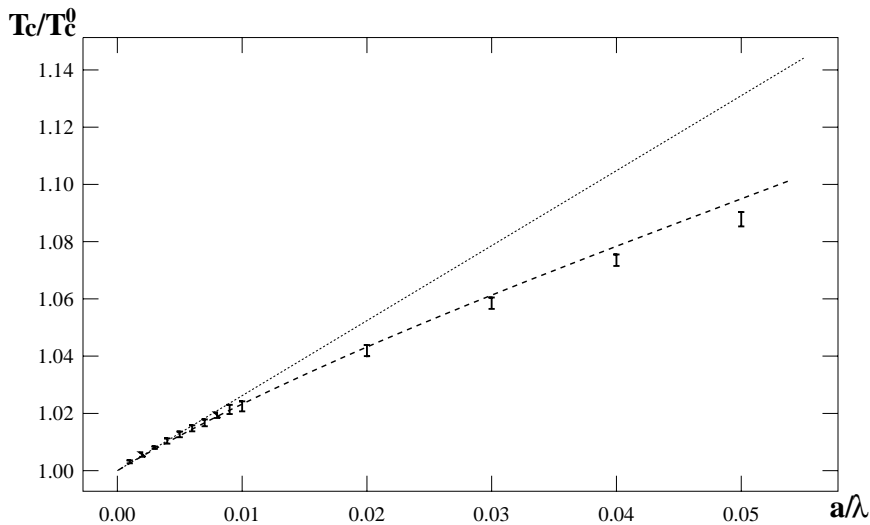


Fig. 6. Dependence of the transition temperature, T_c/T_c^0 , of a dilute homogeneous Bose gas on scattering length a/λ , calculated by solving equations (100, 101) self-consistently. The dashed line is a fit to the data points, given by equation (102). The asymptotic linear behavior extracted from this fit is shown for comparison. The linear behavior is seen only at very small values of a/λ .

5.3.3 Influence of non-zero Matsubara frequencies

Non-linear corrections to the critical temperature shift cannot be obtained within the zero Matsubara frequency sector. One possibility would be to use an effective field theory which includes the effects of non-zero frequencies, *e.g.*, as new vertices in the effective action. Here, we use a different approach, solving the following pair of non-linear equations,

$$\epsilon_k = \frac{\hbar^2 k^2}{2m} + \Sigma(k) - \Sigma(0),$$

$$\Sigma(k) - \Sigma(0) = -2g^2 T \int \frac{d^3 q}{(2\pi)^3} \frac{B(q)}{1 + 2gB(q)} \left(\frac{1}{\epsilon_{k-q}} - \frac{1}{\epsilon_q} \right), \quad (100)$$

where the cutoff in the bubble diagram integral

$$B(q) \simeq \beta \int \frac{d^3 p}{(2\pi)^3} f_p f_{p+q} \quad (101)$$

is no longer a simple step function, but rather the smoother Bose function $f_k = (\exp(\beta\epsilon_k) - 1)^{-1}$. We calculate the shift in the transition temperature using equation (40). Although this does not correspond to a systematic approximation, it provides an illustration of the effect of keeping the full statistical factors in the calculation (instead of using their classical limit).

In Figure 6 we show the calculated critical temperature in the dilute region. The Bose functions in (40) lead to $a^2 \ln a$ corrections in $\Delta T_c/T_c$. On the other hand, the Bose functions in the bubble diagram, equation (101) lead to less singular corrections. We ignore them here and fit the numerical data to the same functional form of equation (99) as in the last subsection, and find,

$$\frac{\Delta T_c}{T_c} \simeq 1.9an^{1/3} \left[1 + 2.6an^{1/3} \ln(3.1an^{1/3}) \right]. \quad (102)$$

Even in the very dilute region, $n^{1/3}a \sim 0.01$, the logarithmic corrections are noticeable and reduce the temperature shift with respect to the linear prediction. This provides a possible explanation for the discrepancy of the different Monte Carlo results [20,23,24] and [19]; whereas references [20,23,24] calculated the linear corrections directly in the limit $n^{1/3}a \rightarrow 0$, reference [19] performed several calculations in the density regime $10^{-6} < na^3 \lesssim 0.1$ finding a shift of the critical density much smaller than expected from the linear formula of references [20,23,24]. Although the logarithmic corrections tend to decrease this linear shift, the approximations underlying equations (100) and (101) are too crude to allow quantitative comparison.

In [15] Bijlsma and Stoof, using renormalization group techniques, obtained an increase of the critical temperature. A peculiar feature of their results is that the dependence of the critical temperature on the dimensionless parameter $an^{1/3}$ is given by an unusual curve, going as $a \ln a$ in the limit of vanishing interaction [17]. The interpretation of such an unexpected dependence is discussed in reference [18].

6 Conclusion

In this paper, we have studied the effects of particle interactions and correlations on the transition temperature for Bose Einstein condensation, and derived the leading effects beyond mean field in dilute systems. Our study is general and not limited to any particular approximation, for instance an arbitrary selection of class of diagrams in a perturbation expansion. We have shown that the leading term in the change of the critical density is first order in the scattering length a , and can be derived by solving

the corresponding classical field theory. Estimating analytically the coefficient requires in general uncontrolled approximations. Among the various approximations that we have tried, our preferred result is the self-consistent calculation of the sum of bubble diagrams, which gives a coefficient 2.0. However this number should not be trusted at a 10% level. Our value is compatible with the most recent numerical results of references [23,24], $c \simeq 1.3$; the complexity of the mathematical problem does not permit one to make a definitive prediction of the prefactor of the linear term from an analytic analysis.

It is remarkable, that, despite this complexity, all approximations that we have used lead to comparable results: to get the right order of magnitude of the critical density or temperature change a precise determination of the energy shift $U(k)$ is not required. The contribution of this function to ΔT_c is actually close to “all or nothing” for extreme k values: for small k , the function is larger than the free particle energy and the corresponding momenta are completely depopulated, the precise value of $U(k)$ is not relevant; for large k , the free particle energy dominates and the value of $U(k)$ is also irrelevant. The important features of $U(k)$ are the crossover value at which it is comparable to the free particle energy spectrum, and the way this region is crossed by the function.

We have limited ourselves to an homogeneous gas contained in a box, ignoring the influence of a possible external potential, for example magnetic traps and optical lattices. In both such systems, the dimensionality can vary continuously from three to two or smaller, and, therefore, affects the nature of the transition. We will discuss them in future publications.

Author GB would like to thank the École Normale Supérieure and the CEA Saclay Center, and GB, FL, and MH the Aspen Center of Physics for hospitality in the course of this work. This research was facilitated by the Cooperative Agreement between the University of Illinois at Urbana-Champaign and the Centre National de la Recherche Scientifique, and supported in part by the NASA Microgravity Research Division, Fundamental Physics Program and by National Science Foundation Grant PHY98-00978 and PHY00-98353. Laboratoire Kastler Brossel de l'École Normale Supérieure is UMR 8552 du CNRS and associé à l'Université Pierre et Marie Curie.

Appendix

Since the formalism of Ursell operators is less common than that of Green's functions, we give in this appendix a few more technical details concerning the equations written in Section 3.1; this will allow the interested reader to make contact with the calculations of reference [21] more easily. For instance, the right side of equation (21) can be obtained from equations (58, 53) and (55) of this reference, which provide:

$$X_k = e^{\beta \Delta \mu} \rho_k, \quad (103)$$

so that (55) becomes:

$$-\log \left[1 - \frac{4a}{\lambda} \left(\frac{\lambda}{2\pi} \right)^3 \int d^3 k \rho_k e^{\beta \Delta \mu} \right]. \quad (104)$$

Equation (21) is then nothing but the first order term in an expansion of this result in powers of a .

Similarly, equation (24) can be obtained as the lowest order expansion of a relation obtained from equations (55, 81) of [21],

$$\beta \delta \mu_k = -\log \left[1 + 8 \left(\frac{a}{\lambda} \right)^2 e^{3\beta \Delta \mu} J_2 \right] \quad (105)$$

with

$$J_2 = \lambda^6 \int \frac{d^3 k'}{(2\pi)^3} \int \frac{d^3 q}{(2\pi)^3} \rho_{k'} \rho_{k'-q} \rho_{k+q} e^{\beta \Delta(k,k',q)}, \quad (106)$$

and

$$\Delta(k, k', q) = \delta \mu_{k'} + \delta \mu_{k'-q} + \delta \mu_{k+q}. \quad (107)$$

We note that we have changed the sign convention of [21] by introducing a minus sign in the right hand side of (24); in this way, positive $\Delta \mu$ as well as positive $\delta \mu_k$ correspond to positive corrections to the self-energies. This convention makes more straightforward the comparison between $\delta \mu_k$ and the self-energy $\Sigma(k)$ introduced in the Green's function formalism.

The exact form of the $\delta \mu$'s is not important for the discussion of Section 3.1. In the context of mean field, what matters actually is only the existence of some k independent form of $\Delta \mu$, and one could use expression (104) as well; nevertheless, it would not improve the accuracy either, since it is, but it is actually just a consequence of the simplest approximation used for the self-consistent equation for ρ . As for correlations effects, the only essential property is the momentum conservation rule that appears in (24) as well as in (106).

Higher orders can be readily incorporated into the self-consistent equation [21]; for instance, a summation of bubble diagrams shown in Figure 3d leads to the generalization of equation (24):

$$\beta(\delta \mu_k - \delta \mu_0) = -4 \frac{a}{\lambda} \lambda^3 \int \frac{d^3 q}{(2\pi)^3} \frac{A(q)}{1 + A(q)} (\rho_{k+q} - \rho_q) \quad (108)$$

where

$$A(q) = 2 \frac{a}{\lambda} \lambda^3 \int \frac{d^3 k'}{(2\pi)^3} \rho_{k'} \rho_{k'-q}. \quad (109)$$

With the factor $A(q)$ in the denominator the integral of equation (108) is convergent in the infrared with a free particle spectrum. Further generalizations are discussed in [21]. Numerical solutions of particular approximations are presented in Section 5. As far as the bubble summation of equation (108) is concerned, we remark that a summation of Ursell ladder-like diagrams leads to the same result without the 2 in the denominator; for more details, see [34].

References

1. G. Baym, C.J. Pethick, Phys. Rev. Lett. **76**, 6 (1996).
2. M. Holzmann, W. Krauth, M. Naraschewski, Phys. Rev. A **59**, 2956 (1999).
3. F. Dalfovo, S. Giorgini, S. Stringari, L. Pitaevskii, Rev. Mod. Phys. **71**, 463 (1999).
4. A.L. Fetter, J.D. Walecka, *Quantum theory of many-particle systems* (McGraw-Hill, 1971), Chap. 28.
5. K. Huang, C.N. Yang, J.M. Luttinger, Phys. Rev. **105**, 776 (1957).
6. T.D. Lee, C.N. Yang, Phys. Rev. **105**, 1119 (1957).
7. T.D. Lee, C.N. Yang, Phys. Rev. **112**, 1419 (1958).
8. A.E. Glassgold, A.N. Kaufman, K.M. Watson, Phys. Rev. **120**, 660 (1960); Appendix B.
9. K. Huang, *Imperfect Bose gas* in *Studies in Statistical Mechanics*, Vol. 2, edited by J. de Boer, G.E. Uhlenbeck (North Holland, 1964).
10. K. Huang, Phys. Rev. Lett. **83**, 3770 (1999).
11. T. Toyoda, Annals of Physics N.Y. **141**, 154 (1982).
12. E.L. Pollock, D.M. Ceperley, Phys. Rev. B **36**, 8343 (1987).
13. D.M. Ceperley, Rev. Mod. Phys. **67**, 279 (1995).
14. H.T.C. Stoof, Phys. Rev. A **45**, 8398 (1992).
15. M. Bijlsma, H.T.C. Stoof, Phys. Rev. A **54**, 5085 (1996).
16. G. Baym, J.-P. Blaizot, M. Holzmann, F. Laloë, D. Vautherin, Phys. Rev. Lett. **83**, 1703 (1999).
17. We thank H.T.C. Stoof for pointing out to us the small a structure of reference [15].
18. M. Holzmann, G. Baym, J.-P. Blaizot, F. Laloë, Phys. Rev. Lett. **87**, 120403 (2001).
19. P. Grüter, D. Ceperley, F. Laloë, Phys. Rev. Lett. **79**, 3549 (1997).
20. M. Holzmann, W. Krauth, Phys. Rev. Lett. **83**, 2687 (1999).
21. M. Holzmann, P. Grüter, F. Laloë, Eur. Phys. J. B **10**, 739 (1999).
22. G. Baym, J.-P. Blaizot, J. Zinn-Justin, Europhys. Lett. **49**, 150 (2000).
23. V.A. Kashurnikov, N.V. Prokof'ev, B.V. Svistunov, Phys. Rev. Lett. **87**, 120402 (2001).
24. P. Arnold, G. Moore, Phys. Rev. Lett. **87**, 120401 (2001).
25. A.M.J. Schakel, Int. Journ. Mod. Phys. B **8**, 2021 (1994); *Boulevard of broken symmetries*, Habilitationsschrift Freie Universität Berlin (1998), `cond-mat/9805152`.
26. M. Wilkens, F. Illuminati, M. Krämer, J. Phys. B **33**, L779 (2000).
27. E. Mueller, G. Baym, M. Holzmann, J. Phys. B (to be published) (2001), `cond-mat/0105359`.
28. F. de Souza Cruz, M.B. Pinto, R.O. Ramos, Phys. Rev. B **64**, 014515 (2001).
29. M. Houbiers, H.T.C. Stoof, E.A. Cornell, Phys. Rev. A **56**, 2041 (1997).
30. P. Arnold, B. Tomášik, `cond-mat/0105147` (2001).
31. J.D. Reppy, B.C. Crooker, B. Hebral, A.D. Corwin, J. He, G.M. Zassenhaus, Phys. Rev. Lett. **84**, 2060 (2000).
32. F. Laloë, *Dilute-degenerate gases in Bose-Einstein condensation*, edited by A. Griffin, D.W. Snoke, S. Stringari (Cambridge University Press, 1995).
33. G. Baym, G. Grinstein, Phys. Rev. D **15**, 2897 (1977).
34. M. Holzmann, Ph.D. thesis, Paris (2000).
35. V. Elser, Ph.D. thesis, University of California, Berkeley (1984).
36. R. Balian, C. de Dominicis, Ann. Phys. **62**, 229 (1971).
37. J.P. Blaizot, G. Ripka, *Quantum theory of finite systems* (MIT Press, 1986).
38. L.P. Kadanoff, G. Baym, *Quantum statistical mechanics* (Benjamin, 1962).
39. A.A. Abrikosov, L.P. Gorkov, I.E. Dzyaloshinski, *Methods of quantum field theory in statistical physics* (Prentice Hall, 1963).
40. A.Z. Patashinskii, V.L. Pokrovskii, *Fluctuation theory of phase transitions* (Pergamon Press, 1979).
41. S.T. Beliaev, Zh. E.T.F. **34**, 151 and 417 (1958); Sov. Phys. JETP **7**, 104 and 289 (1958).
42. A.Z. Patashinskii, V.L. Pokrovskii, Zh.E.T.F. **46**, 994 (1964); Sov. Phys. JETP **19**, 677 (1964).
43. J. Zinn-Justin, *Quantum Field Theory and critical phenomena* (Oxford University Press, 1996).
44. P. Arnold, B. Tomášik, Phys. Rev. A **62**, 063604 (2000).